

A multichannel thiacalix[4]arene-based fluorescent chemosensor for Zn²⁺, F⁻ ions and imaging of living cells

Mao-Qian Ran,^a Jian-Ying Yuan,^a Yuan-Hui Zhao,^a Lan Mu,^a Xi Zeng,^{*a} Carl Redshaw,^b Jiang Lin Zhao^c and

Takehiko Yamato^{*c}

^a Key Laboratory of Macrocyclic and Supramolecular Chemistry of Guizhou Province, Guizhou University, Guiyang 550025, PR China

^b School of Chemistry, University of Hull, Hull, HU6 7RX, UK

^c Department of Applied Chemistry, Faculty of Science and Engineering, Saga University, Honjo-machi 1, Saga-shi, Saga 840-8502, Japan

This is an Accepted Manuscript of an article published by Taylor & Francis in Supramolecular Chemistry on 18 November 2015, available online:

<http://www.tandfonline.com/doi/full/10.1080/10610278.2015.1109645>].

Abstract

The fluorescent sensor **3** based on the 1,3-alternate conformation of thiacalix[4]arene bearing the coumarin fluorophore via an imino group has been synthesized. The sensing properties were evaluated in terms of a colorimetric and fluorescence sensor for Zn²⁺ and F⁻. High selectivity and excellent sensitivity were exhibited, and “off-on” optical behavior in different media was observed. Changes were all visible to the naked eye, whilst the presence of the Zn²⁺ and F⁻ induces fluorescence enhancement and the formation of a 1:1 complex with sensor **3**. In addition, the sensor **3** has low cytotoxicity and good cell permeability, and can readily be employed for assessing the change of intracellular Zn²⁺ and F⁻ levels.

Keywords Thiacalix[4]arene derivative; colorimetric and fluorescent sensor; Zn²⁺; F⁻; cell imaging.

Introduction

Cations and anions are ubiquitous in nature and play critical roles in many biological,

chemical and environmental systems, for example zinc ions are indispensable metal ions in living systems. Zinc-containing proteins are abundant and act as both structural and functional proteins by exhibiting a wide range of biochemical activities.¹⁻⁴ The deficiency of Zn^{2+} ions in the brain and pancreas may result in various disorders such as Parkinson's disease, epilepsy, and certain cancers.^{5, 6} However, an excess dose of zinc can cause several health problems such as superficial skin diseases, prostate cancer, diabetes, and brain diseases.^{7, 8} Supra-optimal zinc concentrations in soil can cause toxicity effects on most of the plants, for instance the inhibition of root elongation and shoot growth.^{9, 10}

On the other hand, amongst the biologically important anions, fluoride is of particular interest owing to its role in preventing dental caries, and in the treatment of osteoporosis. It is a common ingredient in hypnotics, anesthetics, psychiatric drugs and cockroach poisons. Furthermore, excess fluoride ion exposure causes fluorosis, thyroid activity depression, bone disorders and immune system disruption.¹¹⁻¹⁷

As a result of the diversity of their functions, beneficial or otherwise, the development of selective and sensitive methodologies for the detection of zinc and fluoride ions in the environment and in biological samples becomes imperative. Recently, a new method of choice for Zn^{2+} and F^- detection is the use of a colorimetric and fluorescent chemosensor, and this is receiving considerable interest because of its selectivity, sensitivity, and simplicity. Fluorescence sensor molecules allow for the visualization of ion activities in living cells, and are thus useful tools for providing information on the Zn^{2+} and F^- status in living biological systems.¹⁸ Although much progress has been achieved,¹⁹⁻²⁴ sensing multiple analytes with a single chemosensor is still very challenging. Multifunctional sensors for both zinc and fluoride remain rare compared with the variety of sensors developed for other systems.²⁵⁻³²

In the field of calixarene chemistry, a number of new scaffolds/building blocks have emerged for the development of colorimetric and fluorometric chemosensors for multifunctional sensing. Owing to the steric and electronic effect of the bridging sulfur atoms, thiacalixarenes are able of forming a variety of conformations and structures containing cavities that can interact with soft-transition metal ions and

anions. Furthermore, calixarenes/thiacalixarenes can utilize allosteric effects or pre-organization effects to bind different target ions at different times and with different binding sites.³³⁻³⁵

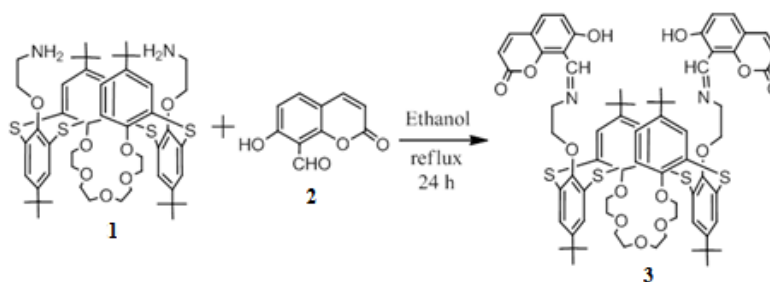
Coumarin is a well known fluorophore which has advantages such as large Stokes shifts, good photo-stability, high fluorescence quantum yields, and readily yields efficient luminescence. Their potential application as fluorescent sensing agents have received much interest.^{36,37} Although significant progress has been made in relation to the detection of Zn^{2+} and F^{-} ions, there are still only a limited calixarene sensors that have been applied to the imaging of living cells. In order to explore the application of thiacalixarenes as potential colorimetric and fluorescent sensors, we envisaged that the introduction of a coumarin aldehyde at a 1,3-alternate thiacalixarene would give rise to a functionalized cavity suitable for sensing multi analytes.

Herein, we report the synthesis of one such 1,3-alternate thiacalix[4]arene derivative containing imino units as binding sites and a 7-hydroxy-8-coumarin formaldehyde moiety as the fluorophore. Such a system possesses notable colorimetric and fluorometric sensing abilities for both cation and anion target ions. It also exhibits cell permeability and intracellular Zn^{2+} and F^{-} sensing in human cancer cell.

Results and discussion

Synthesis of sensor 3

The intermediate compound 1 was synthesized by the reported procedure.³⁸ The condensation of compound 1 with 7-hydroxy-8-coumarin formaldehyde (compound 2) afforded sensor 3; the synthetic route was carried out as outlined in Scheme 1.



Scheme 1 Synthesis of sensor 3

Molecular structure

The IR spectrum of **3** showed a stretching band at 1632 cm^{-1} corresponding to the C=N group. There is no absorption band corresponding to free aldehyde or amino groups, which indicates that the condensation has taken place. The ^1H NMR spectrum of **3** exhibited two singlets (18H each) at δ 1.33 and 1.35 ppm corresponding to the *tert*-butyl protons, six triplets (4H each) at 3.01, 3.17, 3.39, 3.61, 3.95 and 4.12 ppm corresponding to the NCH_2 and OCH_2 protons, four doublets (2H each) at 6.15, 6.77, 7.33, 7.55 ppm corresponding to the aromatic protons of coumarin, two singlet (4H each) at 7.37, 7.45 ppm corresponding to aromatic protons, 8.85 ppm corresponding to the $\text{HC}=\text{N}$ protons and 14.62 ppm corresponding to the OH group. The former four singlets (*tert*-butyl, aromatic protons of the thiacalix[4]arene) for the compound suggested that the sensor **3** possesses a 1,3-alternate conformation with C_{2v} -symmetry.

Study of metal ion binding features

Any UV-Vis changes were observed upon addition of 20 eq. of different metal ions (Li^+ , Na^+ , K^+ , Ca^{2+} , Sr^{2+} , Ba^{2+} , Hg^{2+} , Mg^{2+} , Cu^{2+} , Cd^{2+} , Ni^{2+} , Al^{3+} , Ag^+ , Fe^{3+} , Cr^{3+} , Co^{2+} , and Pb^{2+}) to the solution of **3** ($10\ \mu\text{M}$) in DMF/ H_2O (9/1, v/v), however no significant changes were observed. In contrast, the addition of 20 eq. Zn^{2+} resulted in an obvious change (Fig. 1A); a noticeable colour change from deep yellow to light yellow is readily visible to the naked eye (Fig. 1A, inset), suggesting that **3** showed a specific response to Zn^{2+} ions. The binding ability of **3** towards the Zn^{2+} ion was investigated by UV-vis titration (Fig. 1B). Free **3** exhibited typical absorption bands of coumarin at around 267 nm, 344 nm and 415 nm, and upon addition of increasing amounts of Zn^{2+} (0 ~ 20 μM) to the solution of **3**, the absorbance band at around 267 nm decreased and the band at around 415 nm gradually disappeared, whilst the absorbance bands at 345 nm increased. The presence of the clear isobestic points at 291 nm and 417 nm implies the conversion of the free **3** into the Zn^{2+} complex. From the titration experiments, the association constant for **3**- Zn^{2+} was determined to be $6.98 \times 10^4\ \text{M}^{-1}$ (Fig. S1), the 1:1 binding ratio was confirmed by the Job's plot (Fig. 1B, inset). From the absorption spectra titration, a linear relationship between the

absorbance of **3** and Zn^{2+} concentration (2.0 ~ 12.0 μM , $R = 0.9901$, $n = 8$) was evident, and the detection limit was 7.2 μM (Fig. S2). In order to validate the high sensitivity of **3** toward Zn^{2+} ions, competition experiments were carried out by adding Zn^{2+} ions (20 eq.) to the solution of **3** (10 μM) in the presence of 20 eq. of the previously listed metal ions (Fig. S3). No significant interference was observed in the presence of the various other biologically and environmentally relevant ions, indicating that **3** can be used as a potential probe for Zn^{2+} in the presence of the other competitive species.

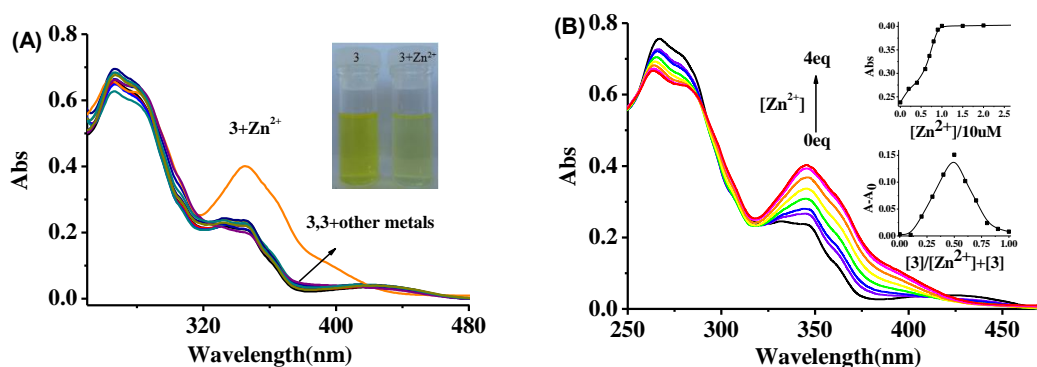


Fig. 1 (A) UV-vis spectra of **3** (10 μM , DMF/H₂O, 9/1, v/v) with 20 eq. of various metal ions. Inset: sunlight images of **3**, **3** and Zn^{2+} . (B) UV-vis spectra titration of **3** (10 μM , DMF/H₂O, 9/1, v/v) with Zn^{2+} . Inset: variation of absorbance against the number of equivalents of Zn^{2+} and Job's plot data. Metal ions: Zn^{2+} , Li^+ , Na^+ , K^+ , Ca^{2+} , Sr^{2+} , Ba^{2+} , Hg^{2+} , Mg^{2+} , Cu^{2+} , Cd^{2+} , Ni^{2+} , Al^{3+} , Ag^+ , Fe^{3+} , Cr^{3+} , Co^{2+} , and Pb^{2+} . $\lambda_{\text{amx}} = 345 \text{ nm}$

Under the same conditions, the fluorescence response of **3** to other metal ions by exciting at 360 nm was tested. On addition of 20 eq. of the previously listed ions, only Mg^{2+} and Ba^{2+} exhibited a slight emission response, whereas the other ions had no obvious effect on the fluorescence emission of **3**. When Zn^{2+} was added to the solution of **3**, a dramatic fluorescent enhancement was observed, suggesting that **3** showed a specific response to Zn^{2+} ions (Fig. 2A). The fluorescent titration was also carried out, in the absence of metal ions, and **3** exhibited a very weak fluorescence peak at 516 nm ($\Phi = 0.0105$, versus quinine sulfate as reference material, $\Phi = 0.55$). This behavior of **3** was probably due to C=N bond *cis*↔*trans* isomerization which may be the predominant decay process in the excited state for **3** with an unbridged C=N

structure.^{39, 40} In contrast, on addition of Zn^{2+} to the solution of **3**, fluorescence enhancement occurred with the emission wavelength clearly shifting from 516 nm to 465 nm. A 56-fold enhancement in the case of the **3**- Zn^{2+} complex was observed ($\Phi = 0.586$), and an obviously bright blue emission could easily be observed by the naked eye (Fig. 2A, inset). This remarkable increase of the fluorescence intensity could be due to the effective coordination of Zn^{2+} with **3** in preference to binding to the other metal ions. The chelation of Zn^{2+} to the oxygen and nitrogen atoms of the phenolic and imine moieties not only increased the rigidity and planarity of the molecular assembly by restricting free rotation of the C=N isomerization process, but also resulted in a large chelation induced enhanced fluorescence (CHEF) effect which induces a large enhancement in the fluorescence. Moreover, it seems to affect the intramolecular charge transfer (ICT) within the sensor.^{41, 42} The electron-donating ability of the phenolic-OH group at one end and electron-withdrawing ability of carbonyl group at another end of coumarin ultimately resulted in a blue shift of the emission spectrum of **3**. The fluorescence titration is shown in Fig. 2B, the nonlinear fitting of the titration curve and the data of the Job's plots from the fluorescence spectra (Fig. 2B, inset) assumed a 1:1 stoichiometry for the **3**- Zn^{2+} complex. The association constant for **3** with Zn^{2+} was calculated to be $3.15 \times 10^4 \text{ M}^{-1}$ using a Benesi-Hildebrand plot (Fig. S4). From the fluorescence spectral titration, there exists a good linear relationship between the emission intensity of **3** and the Zn^{2+} concentration (0.9 ~100 μM , $R = 0.9935$, $n = 10$); the fluorescent detection limit was 43.2 nM (Fig. S5). To check the practical applicability of **3** (10 μM) as a Zn^{2+} selective fluorescent sensor, the competitive experiments were carried out in the presence of Zn^{2+} (20 eq.) at mixed with 20 eq. other metal ions. The results indicated that no significant variation was found in the fluorescence intensity with or without the other metal ions present, the sensing of Zn^{2+} by the sensor was hardly affected by the previously listed metal ions (Fig. S6).

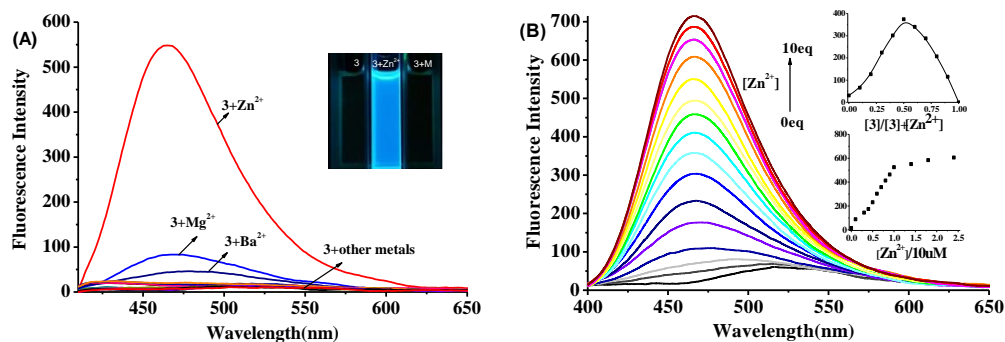


Fig. 2 (A) Fluorescent spectra of **3** (10 μM , DMF/H₂O, 9/1, v/v) with 20 eq. of various metal ions. Inset: fluorescent images of **3**, **3** and Zn²⁺, **3** and other metals. (B) Fluorescent titration of **3** (10 μM , DMF/H₂O, 9/1, v/v) with Zn²⁺ solution. Inset: variation of fluorescence intensity against the number of equivalents of Zn²⁺ and Job's plot data. Metal ions: Zn²⁺, Li⁺, Na⁺, K⁺, Ca²⁺, Sr²⁺, Ba²⁺, Hg²⁺, Cu²⁺, Mg²⁺, Cd²⁺, Ni²⁺, Al³⁺, Ag⁺, Fe³⁺, Cr³⁺, Co²⁺, and Pb²⁺. $\lambda_{\text{em}}/\lambda_{\text{ex}} = 360 \text{ nm}/465 \text{ nm}$.

The binding mode of **3** with Zn²⁺ was examined by ¹H NMR spectroscopy in CDCl₃/CD₃CN (4/1, v/v). The partial ¹H NMR spectra of **3** before and after treatment with various concentrations of Zn(ClO₄)₂ are shown in Fig. 3. Complexation of **3** with Zn²⁺ shifted the proton of the hydroxyl group (He) at δ 14.51 ppm upfield and it gradually disappeared, the imine proton peak (Hf) at 8.82 ppm was downfield shifted by ca. 0.09 ppm and weakened upon complexation. The aromatic protons Hb, Hc, Hd and the Ha protons of the coumarin moiety underwent large downfield shifts of 0.09, 0.09, 0.13 and 0.13 ppm, respectively, due to the reduction of electron density upon coordination to the metal ion. These NMR results suggested that the interaction of **3** with Zn²⁺ ions is via the nitrogen atoms of the imine and the oxygen atoms of the hydroxyl on coumarin.

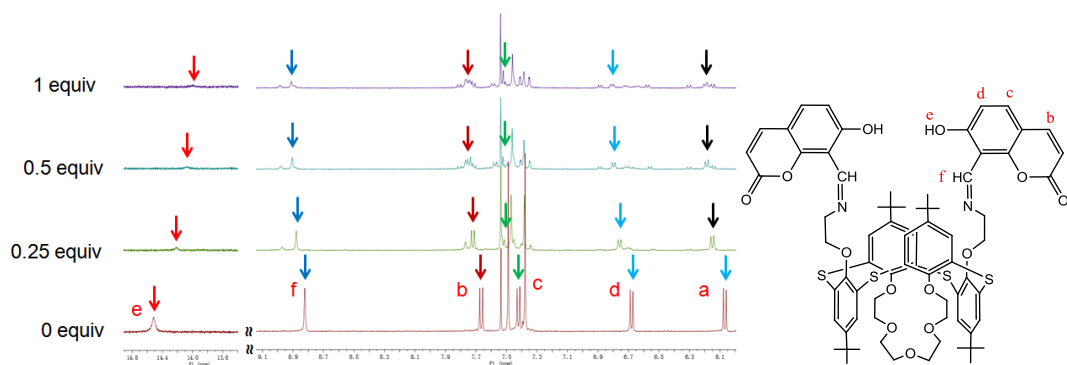


Fig. 3 ^1H NMR spectra in the absence and presence of Zn^{2+} for **3**.

Study of anion binding features

As shown above, **3** contains two hydroxyl groups that could function as anion binding moieties. Hence, we also investigated the sensing properties of **3** toward different anions by fluorescence, absorption and ^1H NMR spectroscopy. Upon the addition of F^- , Cl^- , Br^- , I^- , HSO_4^- , AcO^- , NO_3^- , ClO_4^- , PF_6^- and H_2PO_4^- anions to an CH_3CN solution of **3**, no significant spectral changes were observed in the UV-vis absorption spectra apart from in the case of the F^- ion (Fig. 4). Specifically, the addition of F^- produced a new red-shift absorption band at 390 nm, and “naked-eye” visible color changes from light yellow to deep yellow occurred (Fig. 4A, inset). This observation indicated that **3** is much more selective to F^- ions over other anions screened herein. The absorption spectral titration of **3** with F^- was carried out (Fig. 4B), which revealed that the intensity of the absorption maximum of **3** at around 330 nm gradually decreased while another original absorption band centered at around 416 nm gradually increased and was blue shifted to around 390 nm on increasing the concentration of F^- ion. Also, two well-defined isosbestic points were observed at 348 nm and 436 nm, which suggested complex formation, viz **3-F**. The nonlinear fitting of the titration curve and the data of Job’s plots from the absorption spectra (Fig. 4B, inset) assumed a 1:1 stoichiometry for the **3-F** complex. The association constant for **3** with F^- was calculated to be $3.52 \times 10^4 \text{ M}^{-1}$ using a Benesi-Hildebrand plot (Fig. S7). From the absorption spectral titration, there exists a linear relationship between the absorbance of **3** and the F^- concentration ($0.6 \sim 14 \mu\text{M}$, $R = 0.9939$, $n = 10$); the fluorescent detection limit was $0.53 \mu\text{M}$ (Fig. S8). Competition experiments were also carried out by adding 20 eq. of F^- to the solutions of **3** ($10 \mu\text{M}$) in the presence of other anions. The results indicated that no significant variation was found in the absorbance with or without the other anions present, indeed the sensing of F^- by the sensor was hardly affected by the previously listed anions (Fig. S9).

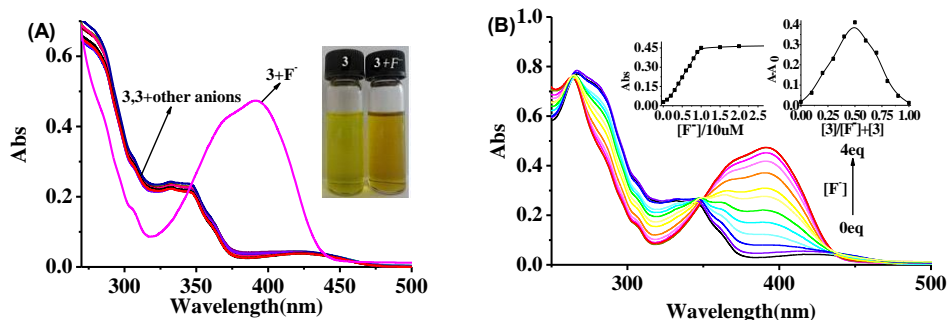


Fig. 4 (A) UV-vis spectra of **3** (10 μM) with 20 eq. of various anions in CH_3CN solution. Inset: sunlight images of **3**, **3** and F^- . (B) UV-vis spectra titrations of **3** (10 μM) with F^- in CH_3CN solution. Inset: variation of absorbance against the number of equivalents of F^- and Job's plot data.

Anions: F^- , Cl^- , Br^- , I^- , HSO_4^- , AcO^- , NO_3^- , ClO_4^- , PF_6^- , and H_2PO_4^- , $\lambda_{\text{max}} = 390 \text{ nm}$

The emission spectra of **3** in the presence of F^- ion was measured in CH_3CN and is shown in (Fig. 5A), and it was found to exhibit fairly weak fluorescence at 500 nm ($\Phi = 0.0187$). After the addition of F^- ion, fluorescence enhancements were observed with a blue shift from 500 nm to 453 nm, and are attributed to the formation of **3**- F^- complexes ($\Phi = 0.512$). The high selectivity of the sensor toward F^- ions is probably due to the formation of multiple hydrogen bonding with the two phenolic OH groups. This binding interaction locks the $\text{C}=\text{N}$ bond of the sensor in place, preventing its rapid isomerisation and switching the fluorescence “on” which also seems to affect the intramolecular charge transfer (ICT) within the sensor resulting in a blue shift and fluorescence color change from non-fluorescence to bright blue (Fig. 5A, inset).^{43, 44} The fluorescence titration (Fig. 5B) also supported these observations, and the association constants which are calculated by data fitting and refining Job's plots suggested that **3** forms a 1:1 complex with F^- (Fig. B inset), with the association constant of $3.08 \times 10^4 \text{ M}^{-1}$ (Fig. S10). From the fluorescence spectral titration, there exists a linear relationship between the emission intensity of **3** and the F^- concentration (3 ~ 11 μM , $R = 0.9984$, $n = 10$); the fluorescent detection limit was 31 nM (Fig. S11). Competition experiments were also carried out by adding 20 eq. of other anions to the solutions of **3** (10 μM). The results indicated that no significant variation was found in the fluorescence intensity with or without the other anions present, in other words, the sensing of F^- by the sensor was hardly affected by the

previously listed anions (Fig. S12).

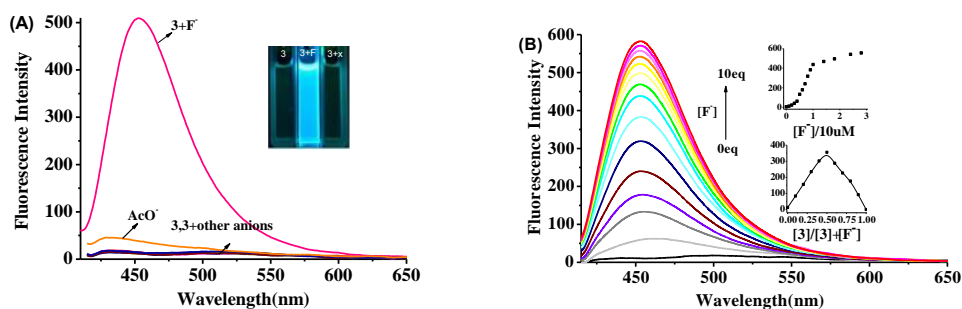


Fig. 5 (A) Fluorescent spectra of **3** (10 μM) with 20 eq. of various anions in CH_3CN solution. Inset: fluorescent images of **3**, **3** and F^- , **3** and other anions. (B) Fluorescent titration of **3** (10 μM) with F^- in CH_3CN solution. Inset: variation of fluorescence intensity against the number of equivalents of F^- and Job's plot data. Anions: F^- , Cl^- , Br^- , I^- , HSO_4^- , AcO^- , NO_3^- , ClO_4^- , PF_6^- , and H_2PO_4^- , $\lambda_{\text{em}}/\lambda_{\text{ex}} = 380 \text{ nm}/452 \text{ nm}$.

In order to pinpoint the anion receptor sites and more fully explore the interaction modes between the anions and sensor molecule, we carried out ^1H NMR titration experiments in $\text{CDCl}_3/\text{CD}_3\text{CN}$ (4/1, v/v) solution. The ^1H NMR spectra of sensor **3** on the addition of F^- is shown in (Fig. 16). Free **3** exhibited a singlet at δ 14.61 ppm corresponding to the OH protons of the coumarin. The peak located at so downfield indicates the formation of intramolecular hydrogen bonding, while the imine ($\text{CH}=\text{N}$) proton gave a singlet at δ 8.84 ppm. The aromatic protons of the sensor resonate in the δ 6.13 ~ 7.57 ppm region. With increasing equivalents of F^- , the signals of He showed progressive upfield shifts. Simultaneously, an upfield shift of the imine proton (Hf) from 8.84 to 8.80 ppm was also observed. This data suggested the formation of a new hydrogen-bonding complex⁴⁵⁻⁴⁷ between **3** and the F^- ion. Simultaneously, the signals due to all other aromatic, methylene and methyl protons were shifted upfield as a result of a through bond propagation effect. However, no characteristic peak was observed in the region of ~ 16.0 ppm due to the formation of an $\text{F}-\text{H}-\text{F}^-$ complex even after the addition of 2 eq. of F^- .^{48, 49} These observations suggest that both -OH groups of **3** are recognizing the fluoride anion through multiple $\text{O}-\text{H}\cdots\text{F}$ hydrogen bonds to form the complex without any deprotonation events. Given this, a mechanism for the

sensing of Zn^{2+} and F^- is proposed in [scheme 2](#).

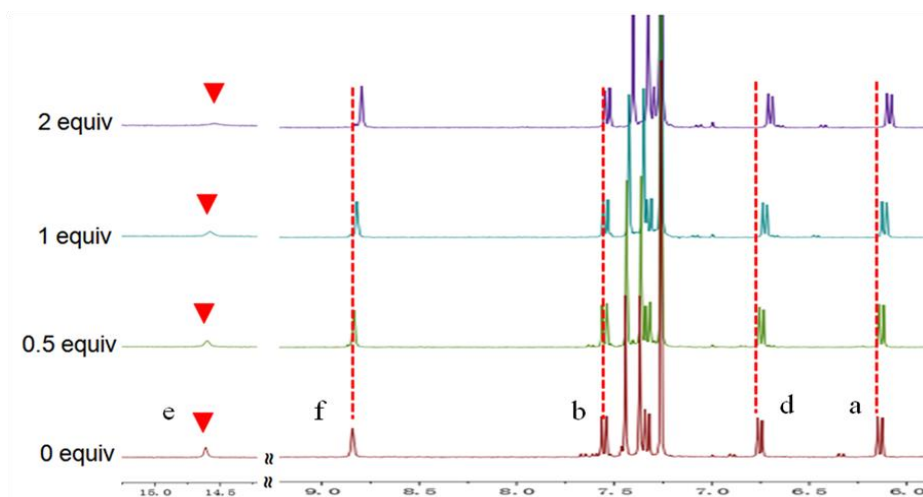
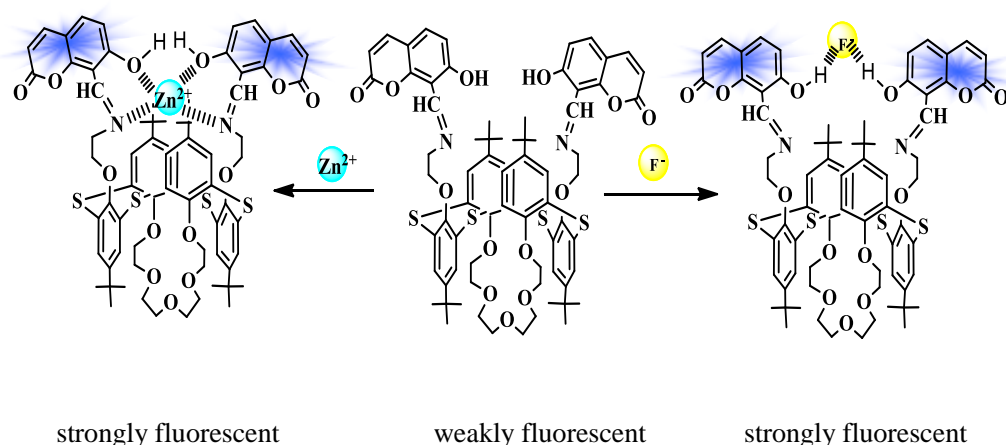


Fig. 6 ^1H NMR spectra of sensor **3** in $\text{CDCl}_3/\text{CD}_3\text{CN}$ (4/1, v/v) in the absence and in the presence of different amounts of F^- .



Scheme 2 Graphic of the proposed mechanism of **3** of Zn^{2+} and F^-

Study of Zn^{2+} and F^- cell imaging

The fluorescence imaging ability of **3** for detecting Zn^{2+} and F^- within living cells was evaluated by using a fluorescence microscope at the blue channel. Incubation of PC3 cells with of **3** ($10\ \mu\text{M}$) for 30 min at $37\ ^\circ\text{C}$ gave almost no intracellular fluorescence as monitored by fluorescence microscopy. [Fig. 7A and 7D](#) were bright-field, [Fig. 7B and 7E](#) were fluorescence measurements which displayed very low intracellular fluorescence. When cells were incubated with growth medium which contained **3** ($10\ \mu\text{M}$) for 30 min, and then underwent the same treatment with of Zn^{2+} ($50\ \mu\text{M}$) for 30

min, remarkable intracellular blue fluorescence (Fig.7C) was generated. When cells were incubated with growth medium which contained **3** (10 μM) for 30 min, and then treated similarly with F^- (50 μM) for 60 min, the cells exhibited highly intense blue fluorescence (Fig. 7F). The fluorescence imaging measurements after treating **3** with Zn^{2+} or F^- confirmed that the merged images support the fact that the fluorescence is being emerged through the cells. Thus, these cellular studies clearly indicate that **3** exhibits good cell permeability and exhibits effective intracellular fluorescence emission through the formation of an *in situ* complex, and can monitor intracellular Zn^{2+} and F^- by *in vitro* imaging and has the potential to be employed *in vivo*.

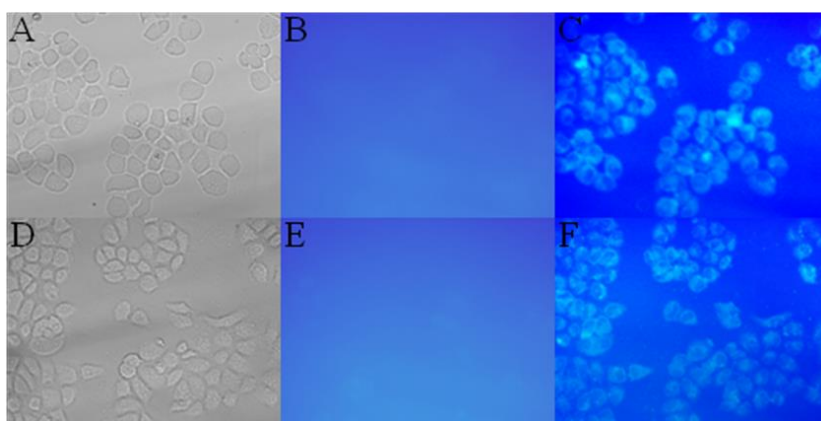


Fig. 7 Fluorescence images of PC3 cells: (A) and (D) bright-field image of cells after incubation with **3** (10 μM); (B) fluorescence image of (A); (E) fluorescence image of (D); (C) blue fluorescence image of **3** (10 μM) treated cells after incubation with Zn^{2+} solution (50 μM); (F) blue fluorescence image of **3** (10 μM) treated cells after incubation with F^- solution (50 μM) from the blue channel

Conclusions

In conclusion, we have synthesized a fluorescent sensor **3** based on a thiacalix[4]arene in the 1,3-alternate conformation, which exhibits a selective fluorescence off-on switchable response towards Zn^{2+} ions in aqueous media, ascribed to the inhibition of the C=N isomerization process and results in a CHEF effect and ICT mechanism. The sensor **3** also exhibits selective off-on fluorescence behavior with F^- , which suggests the formation of hydrogen bonding which suspends the rapid isomerisation and is

accompanied by an ICT process. Furthermore, **3** has suitable permeability into the PC3 cells and can be utilized as a Zn^{2+} and F^- selective sensor in living cells. The sensor **3** is a ditopic receptor based on a thiacalix[4]arene in the 1,3-alternate conformation and possesses a crown-5 moiety as an additional binding site. As a result, allosteric behaviour between $\text{Zn}^{2+}/\text{K}^+$ and F^-/K^+ ions was observed. Thus, sensor **3** may be considered as a potential bifunctional colorimetric and fluorescent sensor for Zn^{2+} and F^- ions.

Experimental

General

Fluorescence spectroscopy measurements were performed on a Cary Eclipse fluorescence spectrophotometer (Varian) equipped with a xenon discharge lamp using a 1cm quartz cell. UV/vis spectra were recorded on a TU-1901 spectrophotometer (Beijing General Instrument Co., China). IR spectra were obtained using a Vertex 70 FT-IR spectrometer (Bruker). Melting points were determined on an X-5 apparatus (Beijing Tech Instrument Co., China) and were uncorrected. ^1H and ^{13}C NMR spectra were recorded on Nova-400 NMR spectrometers (Varian) or a WNMRI-500MHz NMR spectrometer at room temperature, using TMS as an internal standard. MALDI-TOF mass spectra were measured on a BIFLEX III ultra-high resolution Fourier transform ion cyclotron resonance (FT-ICR) mass spectrometer (Bruker) with β -cyano-4-hydroxycinnamic acid as matrix. ESI-MS spectra were recorded on a HPLC-MSD-Trap-VL spectrometer (Agilent). The cell imaging was carried out with an IX-71 inverted fluorescence microscope (Olympus).

Solution preparation

The solutions of the metal ions were prepared from their nitrate salts (Aldrich and Alfa Aesar Chemical Co., Ltd.). All the anions are tetra-butylammonium salts (Sigma-Aldrich Chemical Co.). Other chemicals used in this work were of analytical grade and were used without further purification. Double distilled water was used.

The sensors **3** stock solution (1 mM) was prepared in a 100 mL volumetric flask

with 14.3 mg of sensor **2** was dissolved in absolute THF and DMF.

The Zn^{2+} stock solution (2 mM) was prepared in a 100 mL volumetric flask by dissolving 29.7 mg $\text{Zn}(\text{NO}_3)_2$ in water, and then diluting to the mark with water.

The F^- stock solution (2 mM) was prepared in a 100 mL volumetric flask by dissolving 63.1 mg tetra-*n*-butylammonium fluoride in absolute CH_3CN , and then diluting to the mark with absolute CH_3CN .

The other metal ions were prepared as (2 mM) water solutions; other anions were prepared as (2 mM) CH_3CN solutions.

PC3 cells were grown in Roswell Park Memorial Institute-1640 (RPMI-1640), supplemented with 10% fetal bovine serum, 100 U/mL penicillin and 100 $\mu\text{g}/\text{mL}$ streptomycin at 37 °C and 5% CO_2 . One day before imaging, the cells were seeded in 6-well flat-bottomed plates. The next day, cells were incubated with **3** (10 μM) for 60 min at 37 °C in humidified environment of 5% CO_2 and then washed with fresh culture medium three times to remove the remaining sensor. Before incubating with ion for another 50 min, cells were rinsed with fresh culture medium three times again, and then the fluorescence imaging was observed under inverted fluorescence microscope (excited with UV light). Cells only incubated with **2** (10 μM) for 60 min at 37 °C under 5% CO_2 were as a blank control.

Synthesis of sensor **3**

A solution of 7-hydroxy-8-coumarin formaldehyde (0.12 g, 0.622 mM) in ethanol (20 mL) was added to a solution of compound **1** (0.30 g, 0.311 mM) in ethanol (55 mL) under nitrogen atmosphere. The mixture was refluxed for 24 h, After cooling, the resulting precipitate was filtered and washed with ethanol, and the solid was recrystallized from CHCl_3 -EtOH to give 0.33 mg of sensor **3** as a yellow solid, yield 81.1 %, m.p. 186~188 °C. IR (KBr, cm^{-1}) ν : 3450 (OH), 1742 (C=O), 1632 (C=N), 1242 (C-O-C). ^1H NMR (CDCl_3 , 400 MHz), δ (ppm): 1.33 (s, 18H, $-\text{C}(\text{CH}_3)_3$), 1.35 (s, 18H, $-\text{C}(\text{CH}_3)_3$), 3.01 (t, $J=8.4$ Hz, 4H, NCH_2-), 3.17 (t, $J=7.6$ Hz, 4H, OCH_2-), 3.39 (t, $J=3.6$ Hz, 4H, OCH_2-), 3.61 (t, $J=3.6$ Hz, 4H, OCH_2-), 3.95 (t, $J=7.6$ Hz, 4H, OCH_2-), 4.12 (t, $J=7.6$ Hz, 4H, OCH_2-), 6.14 (d, $J=9.6$ Hz, 2H, Ar-H), 6.76 (d, $J=9.2$ Hz, 2H, Ar-H), 7.34 (d, $J=8.8$ Hz, 2H, Ar-H), 7.37 (s, 4H, Ar-H), 7.45 (s, 4H, Ar-H), 7.56 (d,

$J=9.6$ Hz, 2H, Ar- H), 8.85 (s, 2H, $CH=N$), 14.62 (s, 2H, OH); ^{13}C NMR ($CDCl_3$, 500 MHz), δ (ppm): 31.42, 31.48, 34.40, 34.44, 55.32, 65.57, 66.17, 70.16, 71.40, 73.51, 105.60, 108.83, 111.15, 116.31, 126.44, 127.07, 127.74, 127.84, 132.40, 143.93, 146.87, 146.91, 155.01, 155.13, 156.46, 160.05, 160.27, 169.23; MALDI-TOF MS: m/z 1347.962 $[M+K]^+$. $C_{72}H_{80}N_2O_{13}S_4$ (1308.45): calcd. C 66.03, H 6.16, N 2.14, O 15.88, S 9.79; found C 66.20, H 6.28, N 2.08, O 15.84, S 9.60; (Fig.S13~S16).

Acknowledgments

We are grateful for the financial support from the Natural Science Foundation of China (No. 21165006), the Fund of the International Cooperation Projects of Guizhou Province (No. 20137002), “Chun-Hui” Fund of Chinese Ministry of Education (No. Z2011033, Z2012053). The EPSRC is thanked for the financial support (Overseas Travel award to CR).

References

- 1 E. L. Que, D.W. Domaille, and C.J. Chang, *Chem. Rev.*, 2008, **108**, 1517.
- 2 G. Parkin, *Chem. Rev.*, 2004, **104**, 699.
- 3 W. N. Lipscomb and N. Sträter, *Chem. Rev.*, 1996, **96**, 2375.
- 4 W. Maret, and Y. Li, *Chem. Rev.*, 2009, **109**, 4682.
- 5 N. Omata, T. Murata, N. Maruoka, H. Ikeda, H. Mitsuya, T. Mizuno, K. Mita, M. Asano, Y. Kiyono, H. Okazawa and Y. Wada, *Neurosci. Lett.*, 2012, **531**, 10.
- 6 H. H. Sandstead, *J. Trace Elem. Med. Biol.*, 2012, **26**, 70.
- 7 Y. Xiong, X. P. Jing, X. W. Zhou, X. L. Wang, Y. Yang, X. Y. Sun, M. Qiu, F. Y. Cao, Y. M. Lu, R. Liu and J. Z. Wang, *Neurobiol. Aging*, 2013, **34**, 745.
- 8 S. Ayton, P. Lei and A. I. Bush, *Free Radic. Biol. Med.*, 2013, **62**, 76.
- 9 W. D. Wu, P. A. Bromberg and J. M. Samet, *Free Radic. Biol. Med.*, 2013, **65**, 57.
- 10 R. Terzano, Z. A. Chami, B. Vekemans, K. Janssens, T. Miano, and P. Ruggiero, *J. Agric. Food Chem.*, 2008, **56**, 3222.
- 11 M. Kleerekoper, *Endocrinol. Metab. Clin. North Am.*, 1998, **27**, 441.
- 12 P. d. Beer and P. A. Gale, *Angew. Chem. Int. Ed.*, 2001, **40**, 486.

- 13 C. R. Wade, A. E. J. Broomsgrrove, S. Aldridge and F. P. Gabbaï, *Chem. Rev.*, 2010, **110**, 3958.
- 14 L. S. Kaminsky, M. C. Mahoney, J. Leach, J. Melius and M. J. Miller, *Crit. Rev. Oral Biol. Med.*, 1990, **1**, 261.
- 15 D. Browne, H. Whelton and D. O'Mullane, *J. Dent.*, 2005, **33**, 177.
- 16 R. P. Schwarzenbach, B. I. Escher, K. Fenner, T. B. Hofstetter, C. A. Johnson, U. Gunten, and B. Wehrli, *Science*, 2006, **313**, 1072.
- 17 S. Jagtap, M. K. Yenkie, N. Labhsetwar and S. Rayalu, *Chem. Rev.*, 2012, **112**, 2454.
- [18] Atanu Jana, Pradip K. Sukul, Sushil K. Mandal, Saugata Konar, Sangita Ray, Kinsuk Das, James A. Golen, Arnold L. Rheingold, Sudipa Mondal, Tapan K. Mondal, Anisur R. Khuda-Bukhsh and Susanta K. Kar, *Analyst*, 2014, 139, 495-504.
- 19 R. Joseph and C.P. Rao, *Chem. Rev.*, 2011, **111**, 4658.
- 20 J. S. Kim, and D. T. Quang, *Chem. Rev.*, 2007, **107**, 3780.
- 21 B. S. Creaven, D. F. Donlon and J. McGinley, *Coord. Chem. Rev.*, 2009, **253**, 893.
- 22 S. Patra, R. Lo, A. Chakraborty, R. Gunupuru and D. Maity, *Polyhedron*, 2013, **50**, 592.
- 23 A. Ikeda and S. Shinkai, *Chem. Rev.*, 1997, **97**, 1713.
- 24 P. Lhotak, *Top Curr. Chem.*, 2005, **255**, 65.
- 25 R. K. Pathak, S. M. Ibrahim, C. P. Rao, *Tetrahedron Lett.*, 2009, 50, 2730.
- 26 J. Dessingou, R. Joseph and C. P. Rao, *Tetrahedron Lett.*, 2005, 46, 7967.
- 27 R. Joseph, J. P. Chinta, and C. P. Rao, *J. Org. Chem.*, 2010, 75, 3387.
- 28 R. K. Pathak, K. Tabbasum, A. Rai, D. Panda, and C. P. Rao, *Anal. Chem.*, 2012, **84**, 5117.
- 29 S. H. Lee, H. J. Kim, Y. O. Lee, J. Vicens and J. S. Kim, *Tetrahedron Lett.*, 2006, **47**, 4373.
- 30 H. J. Kim, S. K. Kim, J. Y. Lee, and J. S. Kim, *J. Org. Chem.*, 2006, **71**, 6611.
- 31 V. Bhalla, R. Kumar, M. Kumar and A. Dhir, *Tetrahedron*, 2007, **63**, 11153.
- 32 J. N. Babua, V. Bhallab, M. Kumar and H. Singh, *Lett. Org. Chem.*, 2006, **3**, 787.
- 33 J. S. Kim, O. J. Shon, J. A. Rim, S. K. Kim, and J. Yoon, *J. Org. Chem.*, 2002, **67**, 2348.
- 34 M. Kumar, A. Dhir and V. Bhalla, *Dalton Trans.*, 2010, **39**, 10122.
- 35 Y. Fu, L. Mu, X. Zeng, J. L. Zhao, C. Redshaw, X. L. Ni and T. Yamato, *Dalton Trans.*, 2013, **42**, 3552.
- 36 M. H. Lee, D. T. Quang, H. S. Jung, J. Yoon, C. H. Lee, and J. S. Kim, *J. Org. Chem.*, 2007, **72**, 4242.

- 37 H. Miyaji, H. K. Kim, E. K. Sim, C. K. Lee, W. S. Cho, J. L. Sessler, and C. H. Lee, *J. Am. Chem. Soc.*, 2005, **127**, 12510.
- 38 M. Kumar, A. Dhir and V. Bhalla, *Eur. J. Org. Chem.*, 2009, **26**, 4534.
- 39 J. S. Wu, W. M. Liu, X. Q. Zhuang, F. Wang, P. F. Wang, S. L. Tao, X. H. Zhang, S. K. Wu, and S. T. Lee, *Org. Lett.*, 2007, **9**, 33
- 40 J. Dessingou, R. Joseph and C. P. Rao, *Tetrahedron Lett.*, 2005, **46**, 7967.
- 41 V. Kumar, A. Kumar, U. Diwan and K. K. Upadhyay, *Dalton Trans.*, 2013, **42**, 13078
- 42 S. B. Liu, C. F. Bi, Y. H. Fan, Y. Zhao, P. F. Zhang, Q. D. Luo, D. M. Zhang, *Inorg. Chem. Commun.*, 2011, **14**, 1297
- 43 M. Cametti and K. Rissanen, *Chem. Commun.*, 2009, **45**, 2809.
- 44 B. Liu and H. Tian, *J. Mater. Chem.*, 2005, **15**, 2681.
- 45 M. S. Kumar, S. L. A. Kumar and A. Sreekanth, *Anal. Methods*, 2013, **5**, 6401
- 46 H. Khanmohammadi and K. Rezaeian. *RSC Adv.*, 2014, **4**, 1032
- 47 X. P. Bao and Y. H. Zhou. *Sens. Actuators B: Chem.*, 2010, **147**, 434
- 48 D. Sharma, S. K. Sahoo, S. Chaudhary, R. K. Bera and J. F. Callan, *Analyst*, 2013, **138**, 3646
- 49 D. Esteban-Gómez, L. Fabbrizzi, and M. Licchelli, *J. Org. Chem.*, 2005, **70**, 5717